Patient-specific bone mineral density distribution in the tibia of individuals with chronic spinal cord injury, derived from multi-slice peripheral Quantitative Computed Tomography (pQCT) – a cross-sectional study

Sylvie Coupaud*[1,2], Magnus K. Gislason[1,3], Mariel Purcell[2], Keisuke Sasagawa[4], K. Elizabeth Tanner[5]

1. Department of Biomedical Engineering, Faculty of Engineering, University of Strathclyde, Glasgow G4 0NW, UK;
2. Scottish Centre for Innovation in Spinal Cord Injury, Queen Elizabeth National Spinal Injuries Unit, Queen Elizabeth University Hospital, Glasgow G51 4TF, UK;
3. Institute for Biomedical and Neural Engineering, School of Science & Engineering, University of Reykjavik, Menntavegi 1, 101 Reykjavik, Iceland;
4. Department of Engineering, Niigata Institute of Technology, 1719 Fujihashi, Kashiwazaki City, Niigata 945-1195, Japan;
5. Biomedical Engineering Division, School of Engineering, University of Glasgow, Glasgow G12 8QQ, UK.

* **Correspondence:** Dr Sylvie Coupaud, Department of Biomedical Engineering, Faculty of Engineering, University of Strathclyde, Glasgow G4 0NW, UK. Email: sylvie.coupaud@strath.ac.uk

ABSTRACT

Background: The high risk of fracture associated with chronic spinal cord injury (SCI) is attributed to extensive disuse-related bone loss in previously weight-bearing long bones. Changes in bone mineral density (BMD) after SCI have been documented extensively for the epiphyses of the tibia and femur, fracture-prone sites in this patient group. Less attention has been given to patterns of cortical bone loss in the diaphyses, but variability in BMD distributions throughout the long bones may contribute to some patients' increased susceptibility to shaft fractures in chronic SCI.

Aim: A cross-sectional study was carried out to determine whether BMD distributions along the tibia differ between individuals with chronic SCI and healthy able-bodied (AB) controls, in both the trabecular and cortical bone compartments. The effects of time post-injury and gender on BMD distribution were also explored.

Methods: Individuals with chronic (≥ 6 months post-injury) motor-complete SCI were recruited from the Queen Elizabeth National Spinal Injuries Unit (Glasgow, UK). AB control subjects were recruited to achieve similar age and gender profiles for the SCI and control groups. Multi-slice pQCT (XCT3000, Stratec) was performed along the length of the tibia (2mm thickness, 0.5mm voxel size), at 1% intervals in the epiphyses and 5% intervals in the diaphysis (34 slices in total). These were used to reconstruct full 3-D subject-specific models (Mimics, Materialise) of BMD distribution, by interpolating between slices. Subjects with chronic SCI were subdivided into 'early' (<4 years post-injury) and 'established' SCI (≥4 years post-injury). Subject-specific BMD distribution was described according to new parameters determined from the 3-D patient-specific models, quantifying descriptors of the trabecular and cortical BMD regions separately (volume, peak BMD, half-peak width, area under the curve). These were compared between sub-groups (using independent-samples t-tests or Mann-Whitney tests, significance level of 5%).

Results: 11 men (age range 17-59 years old; mean 35.7±10.6) and 3 post-menopausal women (age range 56-58 years old; mean 56.7±1.2 years) with motor-complete SCI (ranging from 6 months to 27 years post-injury) were recruited; 6 men (age range 20-56 years old; 33.0±12.7 years) and 1 post-menopausal woman (56 years) formed the AB control group. Overall, SCI resulted in lower BMD at both trabecular and cortical regions of the tibia. In men, longer time since injury resulted in greater BMD differences when compared to AB, throughout the tibia. For the post-menopausal women, differences in BMD between SCI and AB were greater in cortical bone than in trabecular bone. From the models, individual BMD distribution curves showed healthy double-peaks in AB subjects: one trabecular peak (around 200-300 mg/cm^3) and the other cortical (around 1000-1100 mg/cm^3). In most subjects with established SCI, trabecular peaks were exaggerated whilst the cortical peaks were barely discernible, with crucially some individuals already exhibiting a diminishing cortical BMD peak, less than 4 years post-injury.

Conclusions: These findings may have implications for determining the fracture susceptibility of the long bones in individual patients with SCI. Epiphyseal fractures associated with low trabecular BMD are well characterised, but our data show that some individuals with SCI may also be at higher risk of shaft fractures. The proposed BMD distribution description parameters, determined from patient-specific models, could be used to identify patients with a weakened diaphysis who may be susceptible to fractures of the tibial shaft, but this requires validation.

1. INTRODUCTION

Chronic spinal cord injury (SCI) provides a natural example of bone's adaptation to reduced loading, typically referred to as disuse osteoporosis. Paralysis of the leg muscles, dependence on a wheelchair for mobility, and a general sedentary lifestyle produce a sudden decrease in the mechanical loading of the long bones, and the resulting bone loss can be rapid and extensive. A number of studies have described an exponential time-course of decline in bone mineral density (BMD) in the cancellous (trabecular) regions of the long bones, mainly at the epiphyses of the tibia and femur **[1,2]**. The trabecular BMD can take between three and seven years to stabilise at a new, lower steady-state; it is not unusual for this chronic SCI steady-state BMD to be below 50% of the pre-injury healthy values. Disuse osteoporosis also manifests itself in compact (cortical) bone through a thinning of the shaft rather than a decrease in BMD; although recent evidence from a longitudinal study shows significant decreases in cortical BMD in the first year post-SCI **[3]**, this decrease may be transient **[4]**. With time, in the diaphyses, the cortical thinning that leads to a weakening of the shaft of the long bones appears to occur mostly through endocortical resorption **[1,5]**. These are the two main adaptations of the long bones to reduced mechanical loading associated with extensive muscle paralysis below the level of the SCI. However, studies by Coupaud *et al.* **[6]** and Gislason *et al.* **[7]** suggest a spectrum of spatio-temporal patterns of bone loss exhibited by different people after a complete SCI. These different spatio-temporal patterns have been described and mapped statistically using custom-made image processing techniques **[8]** and morphometry-based shape models **[9]**.

The clinical significance of the variability of these spatio-temporal patterns of bone loss after SCI is the scope for tailoring the treatment of bone loss in patients with SCI, according to the specific structural weaknesses in different areas of the long bones and treatment needs of the individual. The patient-specific treatment strategy would take into account the extent of bone deterioration in the different compartments of the bone structure (epiphyseal and/or diaphyseal), the phase of bone loss that the person is in (early SCI, chronic SCI, established osteoporosis), the overall musculoskeletal health of the individual, and other factors (e.g. age) that may affect his/her potential to respond to treatment. The choice of treatment, whether physical (exercise, therapy), pharmacological (e.g. anti-resorptive or anabolic therapy), or a combination of the physical and pharmacological interventions, would be a clinical decision informed by an analysis of the individual's relevant risk factors for rapid osteoporosis progression and future fractures.

There is a high risk of fracture in the long bones of individuals with chronic SCI that is associated with weakened osteoporotic bone. In chronic SCI, the incidence of fracture is at least twice as high as in the general population **[10]**. Furthermore, these are fragility fractures that can result from everyday activities or low-force events, and so are related to the weakness of the bone structure as well as the direction and magnitude of loading that leads to the catastrophic failure (fracture) of the bone. This is evidenced from the fact that typical fracture locations in chronic SCI coincide with areas of weakness in the long bones that exhibit disuse osteoporosis, i.e. around the knee (distal

femur, proximal tibia) and above the ankle (distal tibia), the same regions of extensive epiphyseal bone loss in many people with SCI. The typical locations of fractures match the patterns described in our recent publication highlighting low BMD in epiphyseal regions of the tibia as being a consistent feature of bone weakening in chronic SCI **[7]**. In contrast, there was considerable variability between subjects observed in the patterns of cortical bone loss in the tibial diaphysis. Compared to epiphyseal fractures, fewer fractures are recorded in the shafts of the long bones in people with chronic SCI **[11,12,13]**. Patterns in cortical bone can vary considerably between individuals, with some patients appearing to have tibial shafts as dense as those of able-bodied subjects. These differences can be quantified by using a bone imaging technique of adequate resolution to develop computational model representations of each subject's own tibia.

By using peripheral Quantitative Computed Tomography (pQCT), sufficient detail can be collected about the distribution of bone mineral along the length and cross-section of the bone (longitudinal and transverse axes) to build a detailed map of the BMD distribution and bone geometry of each individual's bone. With pQCT these can be quantified separately for trabecular and cortical bone. Data from multi-slice pQCT scans taken along the length of the tibia in persons with SCI and able-bodied (AB) control subjects allow for personalised models of BMD distribution. Using 3-dimensional models that include patient-specific imaging-based data, this study aims to determine to what extent the distribution of BMD along the entire length of the tibia differs between individuals with SCI and control subjects. In addition, the study explores the effects of gender and time since injury on the patterns of BMD distribution.

2. MATERIALS AND METHODS

2.1 Subjects

Candidates eligible for inclusion in the SCI group were identified by physicians at the Queen Elizabeth National Spinal Injuries Unit (QENSIU), in Glasgow (Scotland, UK). Able-bodied (AB) control subjects were recruited by poster advertisement in the workplace. Inclusion criteria for the SCI group were: men (16+) or post-menopausal women (minimum age 55 years) with motor-complete SCI at neurological levels C4 and below. Exclusion criteria were: ventilator-dependency, recent fracture(s) in the limb to be scanned, excessive spasticity, skin sores/pressure ulcers resulting in the person being unable to withstand 3 hours lying down on the scanner bed. AB control subjects were recruited to achieve a similar age-profile as for the SCI group. The main additional exclusion criterion for AB subjects was previous diagnosis of relevant bone conditions (e.g. osteoporosis). Subjects with SCI were recruited first. Based on the age and gender profile of the SCI group, AB subjects were recruited for inclusion in the control group such that a similar AB age and gender profile was produced. No power calculation was performed to determine the sample sizes for this exploratory cross-sectional study. Ethical approval for the study was provided by the NHS West of Scotland Research Ethics Committee for Greater Glasgow & Clyde. Subjects provided informed consent prior to taking part in the study, in accordance with the Declaration of Helsinki.

2.2 Protocol

Scans were performed at the QENSIU by a single operator (SC), using a peripheral Quantitative Computed Tomography (pQCT) scanner (XCT3000, Stratec Medizintechnik, Germany). Unilateral multi-slice pQCT scans of the tibia were carried out along the length of the dominant lower leg, unless the subject had a recent history of fracture on that side, in which case the non-dominant leg was scanned. Prior to each multi-slice scan, a quality assurance (QA) scan was performed using the manufacturer's phantom. The QA scan is not a calibration, but checks measured BMD values against calibrated values. Due to the limitations in the scanning distance achievable with the equipment, the tibia was scanned in two sections, the distal portion followed by the proximal portion, starting at the epiphysis in both cases. For each section, a scout view was performed initially to identify the joint gap (ankle or knee). In most cases, the distal and proximal scan sets consisted of 17 images each, leading to a total of 34 images of the tibia, per subject. Images were taken at 1% intervals in the epiphyseal regions and at 5% intervals in the diaphyseal regions of the tibia (where 100% = total bone length). A polyethylene rod was attached along the side of the lower leg during scanning; this fiducial marker was then used to align the distal and proximal sets of scans, for 3D modelling of the entire tibia. The pQCT images were taken with a 0.5mm voxel edge length, and 2mm image slice thickness.

2.3 pQCT Outcome measures

The manufacturer's software (XCT550, Stratec Medizintechnik, Pforzheim, Germany) was used to calculate standard pQCT bone outcome measures, validated for use in patients with SCI **[1,2,3,4,14]**. A threshold peel (XCT550 contour mode C1; peel mode P1) was used to delineate the trabecular bone in epiphyseal images by removing the outer layer of cortical bone, thus reducing voxelation effects in calculating trabecular BMD. The threshold used for trabecular bone was 180 mg/cm^3 for the distal tibia and 150 mg/cm^3 for the proximal tibia. For diaphyseal images, a threshold peel for cortical bone was set at 710 mg/cm^3, which has been shown to be appropriate for both AB and SCI populations **[14]**. Cross-sections at each of four key sites along the tibia were analysed for total and trabecular or cortical BMD: namely, distal epiphysis (4%), distal diaphysis (14%), mid-shaft (38%), proximal shaft (66%) and proximal epiphysis (96%).

2.4 Modelling protocol

Using multi-slice pQCT, a compromise was reached between the number of images acquired and the total scan time (and radiation dose) per session. The 34 images (each 2mm thick) taken per subject only accounted for a total of 78mm of scanned bone, compared to a total bone length ranging from 350-450mm, thus, approximately 20% of tibial bone length (range 17-22%). Therefore, interpolation between slice locations was performed to create full 3D models of each subject's tibia. For this, image stacks were converted to BMP files and imported into Mimics (Materialise), and interpolation algorithms were used to create 3D volume meshes based on image slices. To

compensate for the coarse slice thickness in the models, resampling was performed at a constant 1% slice thickness throughout the overall length of the bone, as described in Gislason *et al.* **[7]**. This resulted in a subject-specific full-length tibia model, based on each individual's multi-slice pQCT data. The maximum BMD for each subject was identified and, using linear interpolation, each element was converted into a density value.

2.5 Modelling outcome measures

For each subject, the BMD distribution for the whole bone was calculated using the linear relationship between greyscale and density. The material properties for each bone were defined as a set of 100 material densities ranging from below the minimum density value measured in any of the bones to above the highest determined from the linear interpolation. This gave a range of 1200 mg/cm^3 which was divided into 100 equal steps of 12 mg/cm^3. The volume of each tetrahedral element was calculated using the formula:

$$V = \frac{1}{6}\det\left(\begin{bmatrix} 1 & 1 & 1 & 1 \\ x_1 & x_2 & x_3 & x_4 \\ y_1 & y_2 & y_3 & y_4 \\ z_1 & z_2 & z_3 & z_4 \end{bmatrix}\right)$$

Where x, y and z represent the coordinates of each of the four node points. The total volume of elements at each BMD value was calculated and analysed. For each subject, a peak was detected at the low BMD spectrum, where most of the voxels associated with the trabecular bone region exist, and in most cases another peak was detected towards the high BMD cortical region. The trabecular and cortical BMD peaks were located automatically to quantify the number of voxels assigned to each of the relevant BMD ranges (see Figure 1). The full width at half maximum region was defined, and a spline curve was fitted through the full width at half maximum. The following variables were calculated for each of the cortical and trabecular bone regions:

- The peak BMD (in mg/cm^3)
- The peak volume (in cm^3)
- The width at half maximum (in mg/cm^3)
- The normalised area under the curve (AUC) for the region (in mg, and as a % of total AUC).

2.6 Statistical analysis

Descriptive statistics were used to determine the group demographics for the SCI and AB control groups. After testing data for normality, independent samples t-tests were used to quantify differences in BMD and bone geometries between the male subjects with SCI and male AB controls for the scan sites selected for analysis. Due to the small numbers of female subjects, differences in bone parameters between male and female subjects were tested using the non-parametric Mann-Whitney test. All statistical tests were carried out using SPSS (version 20.0, IBM), with a significance level for all analyses set at 5%.

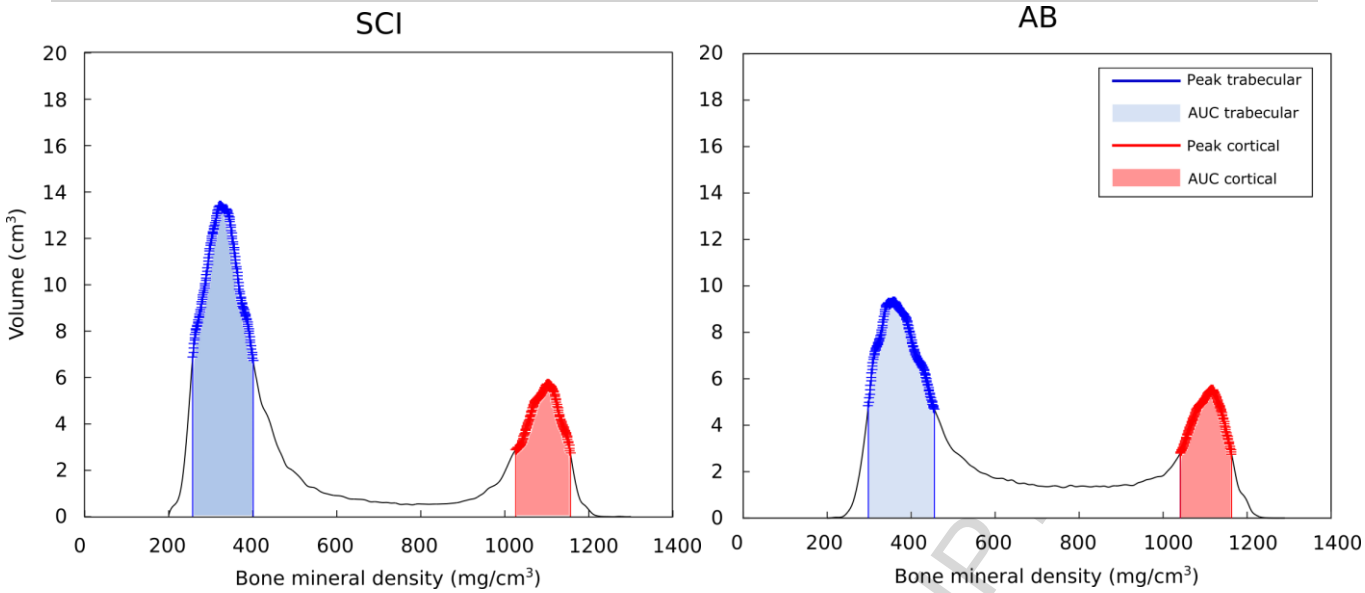

Figure 1: Volume of elements (in cm^3) across the range of BMD values (in mg/cm^3) for representative subject-specific tibia models. These distributions are based on each individual's own multi-slice pQCT scans; fitted curves for the trabecular (blue) and cortical (red) portions of the bone are superimposed. SCI: spinal cord injury; AB: able-bodied; AUC: area under the curve.

3. RESULTS

3.1 Study participants

11 men and 3 post-menopausal women with chronic SCI, ranging from 6 months to 27 years post-injury, were recruited to the SCI group; 6 men and one post-menopausal woman were recruited to the AB control group. Due to the possible confounding effect of gender, and small numbers of post-menopausal female participants, data are presented separately for male and female subjects. Age was comparable between within-gender subgroups: male SCI (n=11, 35.7±10.6 years), male AB (n=6, 33.0±12.7 years); post-menopausal female SCI (n=3, 56.7±1.2 years), post-menopausal female AB (n=1, 56 years). To distinguish between individuals likely to be at bone steady-state from those whose BMD was expected to be in a phase of bone loss (according to the time-course of bone loss described in the cross-sectional study by Eser *et al.* (2004) **[1]**), subjects with chronic SCI were allocated to subgroups according to time since injury: early SCI (between 6 months and 4 years post-SCI) or established SCI (≥ 4 years post-SCI).

3.2 pQCT Images

A number of pQCT images and datasets could not be included in the analysis due to excessive movement artefact, typically resulting from spasticity **[14,15]**. For 3 subjects, the artefacts caused issues of misalignment of images for reconstruction in the models, and so full tibia models could not be created. Thus, full models were available for 13 subjects with SCI and 7 AB control subjects. Representative pQCT images of the distal (4%, 14%, 38%) and proximal

(66%, 96%) scan sites are shown in Figure 2. These illustrate qualitative differences in the patterns of bone loss exhibited by different subjects with SCI, at different times post-injury, compared to AB subjects.

3.3 Bone quality parameters

BMD and patient-specific modelling outcome measures are presented separately for each of the subgroups: (a) early SCI (<4 years post-injury), n=6 male, n=3 female; (b) established SCI (≥4 years post-injury), n=5 (all male), and (c) AB controls, n=6 male, n=3 female. Where relevant, data are presented separately for men and post-menopausal women (Tables 1 & 2). For male subjects, BMD data calculated for selected image slices for trabecular bone in the distal and proximal epiphyses, and for cortical bone in the diaphyses (for three slices in the tibial shaft) are compared between the three subgroups (Table 1). The selected slice locations coincide with the standard 4-slice tibial set recommended by the manufacturers (Stratec Medizintechnik, Pforzheim, Germany). These slice locations are at 4%, 14%, 38% and 66% of total bone length (in relation to the distal reference point). Data from an additional slice at 96% are compared between groups because it is a clinically-relevant site: the proximal tibia epiphysis is prone to fracture in chronic SCI.

Table 1: Average BMD for **male subjects** in the trabecular regions (distal and proximal epiphyses), and in the cortical regions of the tibial shaft (diaphysis). These are given as mean +/-SD separately for Established SCI (≥ 4years post-injury), Early SCI (<4 years post-injury) and AB controls. (* n=5 for this group at this site, as excessive spasticity precluded all relevant slice locations from being imaged).

Subject group	**Bone Mineral Density (BMD), in mg/cm^3**				
Male subjects	Trabecular BMD at distal epiphysis (4%)	Cortical BMD at distal diaphysis (14%)	Cortical BMD at mid-diaphysis (38%)	Cortical BMD at proximal diaphysis (66%)	Trabecular BMD at proximal epiphysis (96%)
Able-bodied (AB) N=6	283.5 ± 52.9	1145.1 ± 29.8	1170.5 ± 26.8	1122.8 ± 19.9	193.8 ± 32.8
Early SCI N=6	178.3 ± 96.0	1106.0 ± 20.7*	1123.0 ± 20.8	1063.7 ± 50.1	112.0 ± 40.9
Established SCI N=5	93.9 ± 40.8	1038.1 ± 131.2	1060.1 ± 131.1	1020.0 ± 76.4	76.2 ± 40.0

Mann-Whitney tests revealed that there were no significant differences in BMD (trabecular or cortical) or cortical cross-sectional area (CSA) between male and female subjects (p-values ranging from 0.172 to 1.000) at the selected image locations. Comparing the median BMD and geometry parameters between the SCI and AB groups showed statistically significant differences in trabecular BMD (p=0.007 for distal tibia; p=0.001 for proximal tibia) and cortical BMD (with p-values ranging from 0.001 to 0.014) at diaphyseal sites. There was no significant difference in cortical CSA between SCI and AB groups (data not shown).

Table 2: BMD for post-menopausal **female subjects** in the trabecular regions (distal and proximal epiphyses), and in the cortical regions of the tibial shaft (diaphysis). These are given as mean +/-SD for Early SCI (<4 years post-injury). There were no female subjects with Established SCI.

Subject group	**Bone Mineral Density (BMD), in mg/cm^3**				
Female subjects	Trabecular BMD at distal epiphysis (4%)	Cortical BMD at distal diaphysis (14%)	Cortical BMD at mid-diaphysis (38%)	Cortical BMD at proximal diaphysis (66%)	Trabecular BMD at proximal epiphysis (96%)
Able-bodied (AB) N=1	228.6	1103.7	1125.8	1090.5	169.9
Early SCI N=3	213.4 ± 59.3	974.1 ± 113.7	1085.9 ± 70.4	1042.8 ± 61.5	140.4 ± 62.0

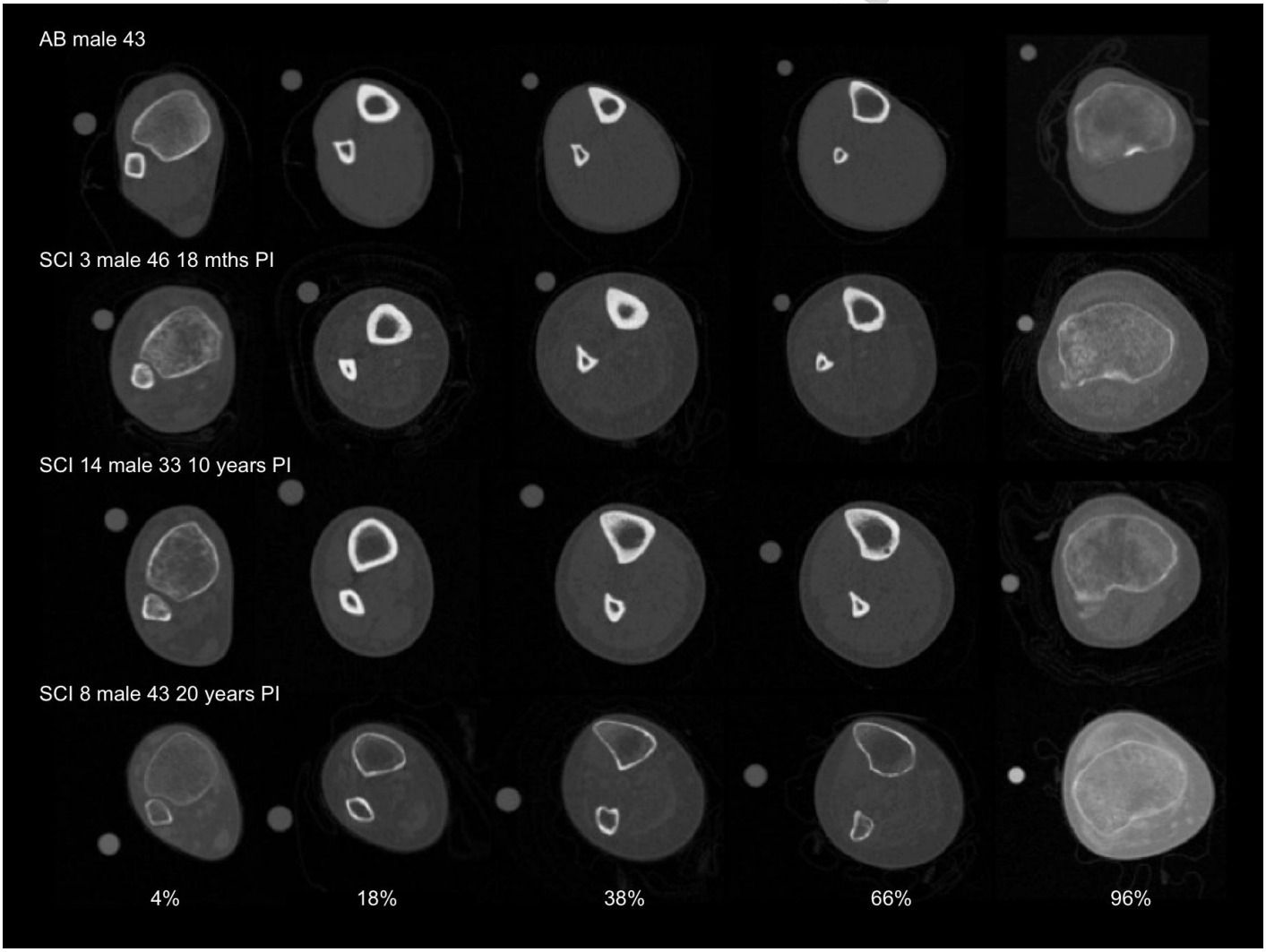

Figure 2: Examples of greyscale pQCT images at selected locations along the left tibia in 1 AB and 3 SCI subjects (at different times post-injury), from left to right: distal epiphysis (4%), distal shaft (14%), mid-shaft (38%), proximal shaft (66%) and proximal epiphysis (96%). Top to bottom: AB 3 (male, 43 years old); SCI 3 (male, 46 years old, 18 months post-injury); SCI 14 (male, 33 years old; 10 years post-injury); SCI 8 (male, 43 years old, 20 years post-injury). The polyethylene fiducial marker can be seen to the left of each image.

3.4 Modelling results

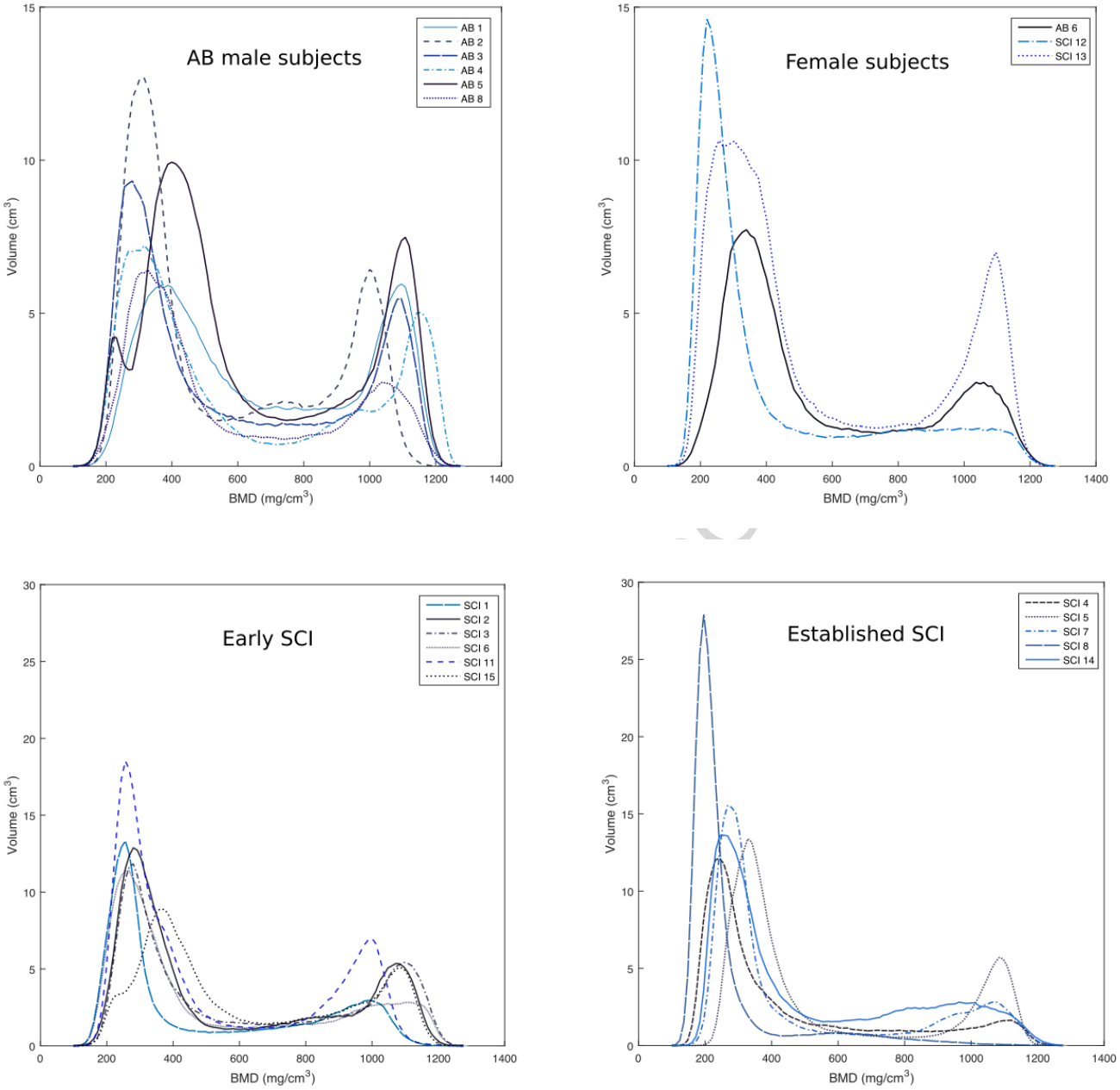

Figure 3: Volume of model elements assigned to the range of BMD values in the subject-specific 3D tibia models, based on multi-slice pQCT. Top left: Male AB subjects (control group); top right: female subjects (one AB and two with early SCI); bottom left: male subjects with SCI (early SCI); bottom right: male subjects with SCI (established SCI).

3.5 Sub-group comparisons

Some patterns emerge when comparing AB, early SCI and established SCI sub-groups (Tables 3 & 4, for male subjects only). Firstly, on average, the peak volume of tibia model elements assigned BMD values in the **trabecular** BMD range is almost twice as high in established SCI as in AB controls, with an intermediate peak magnitude in early SCI. Independent-samples t-tests reveal that the difference between AB and SCI groups is significant (p=0.030 for AB versus early SCI; p=0.021 versus established SCI). There is no significant difference in peak trabecular volume between early and established SCI, but there is a trend for a gradual increase from AB to established SCI. The peak

volume of tibia model elements in the **cortical** BMD range in established SCI is almost half that of AB, and this difference is statistically significant (p=0.026). The cortical peak volume in the early SCI group is intermediate in magnitude between the AB and established SCI cortical peaks.

The half-peak width, which describes the spread of BMD around each region peak (trabecular and cortical, separately), is significantly different between AB and early SCI for the trabecular bone region (p=0.022). For cortical bone, the half-peak width is not significantly different between any of the sub-groups but there is a trend for this value to increase gradually with time since injury. The lack of significance in the cortical region could be attributed to (i) a large standard deviation for cortical peak width, and/or (ii) the inability of the algorithm to detect a true cortical 'peak' in some of the subjects with SCI.

The trabecular area under the curve (AUC) as a percentage of total AUC increases significantly from early to established SCI (p=0.019) and is smaller in AB compared to established SCI (p=0.046). The lack of significance of the difference between sub-groups for cortical AUC may be related to the large SD of the mean for established SCI. The trabecular peak BMD is significantly lower in established SCI compared to AB (p=0.024).

For female subjects, the small numbers preclude firm trends from being described, hence no statistical analyses were performed to compare the post-menopausal women with SCI and the post-menopausal AB control subject. However, Figure 3 shows that, of two female subjects with early SCI, one has a distinct cortical peak (even more so than the AB control subject) whilst the other already shows the trabecular skew more typical of established SCI.

Table 3: BMD distribution along the length of the subject-specific tibia models, for **male subjects** only, quantified for the **trabecular bone** regions. These are presented as mean +/-SD for Established SCI (≥ 4years post-injury), Early SCI (<4 years post-injury) and AB controls. (AUC: Area Under the Curve)

Male subjects	**Trabecular peak volume (cm^3)**	**Trabecular ½-peak width (mg/cm^3)**	**Trabecular AUC (mg)**	**Percentage trabecular AUC (%)**	Trabecular **peak** BMD **(mg/cm^3)**
AB N=6	8.59 ± 2.59$^{§~}$	210.68 ± 51.01§	1414.99 ± 243.55	43.32 ± 2.46$^{~}$	337.00 ± 47.65$^{~}$
Early SCI N=6	12.84 ± 3.20§	145.02 ± 30.41§	1424.01 ± 229.76	40.89 ± 3.95$^{\$}$	282.68 ± 40.56
Established SCI N=5	16.55 ± 6.47$^{~}$	119.93 ± 28.01	1504.54 ± 179.70	49.64 ± 6.19$^{\$~}$	257.15 ± 49.71$^{~}$

§ Significant difference (p<0.05) between early SCI and AB; $^{\$}$ significant difference between established SCI and early SCI; $^{~}$ significant difference between established SCI and AB.

Table 4: BMD distribution along the length of the subject-specific tibia models, for **male subjects** only, quantified for the **cortical bone** regions. These are presented as mean +/-SD for Established SCI (≥ 4years post-injury), Early SCI (<4 years post-injury) and AB controls. (AUC: Area Under the Curve)

Male subjects	Cortical peak volume (cm^3)	Cortical ½-peak width (mg/cm^3)	Cortical AUC (mg)	Percentage cortical AUC (%)	Cortical peak BMD (mg/cm^3)
AB N=6	5.53 ± 1.60$^{\sim}$	154.64 ± 38.31	649.34 ± 121.89	19.89 ± 2.07	1081.00 ± 51.82
Early SCI N=6	4.79 ± 1.61	220.06 ± 88.35	747.35 ± 113.26	21.50 ± 2.45	1058.36 ± 51.42
Established SCI N=5	2.69 ± 1.96$^{\sim}$	251.06 ± 111.69	487.59 ± 290.49	15.45 ± 8.05	1008.28 ± 129.70

§ Significant difference ($p<0.05$) between early SCI and AB; $^{\$}$ significant difference between established SCI and early SCI; $^{\sim}$ significant difference between established SCI and AB.

3.6 Patient-specific model outcomes

Although group comparisons describe the trends in changes in BMD distribution after SCI, away from the healthy 'double-peak' BMD distribution and moving instead towards a low-BMD skew in the trabecular bone BMD range (around 200-300 mg/cm^3), attention should be paid to each patient's own BMD distribution and the extent of his/her deviation from the normal double-peak pattern. In particular, three subjects with early SCI – SCI1, SCI6, and SCI12 (Figure 4) – already showed evidence of losing the cortical BMD peak at around 1000-1200 mg/cm^3, and exhibited instead a skew in the trabecular BMD range (200-300 mg/cm^3). Overall, this pattern was more typical of those with established SCI.

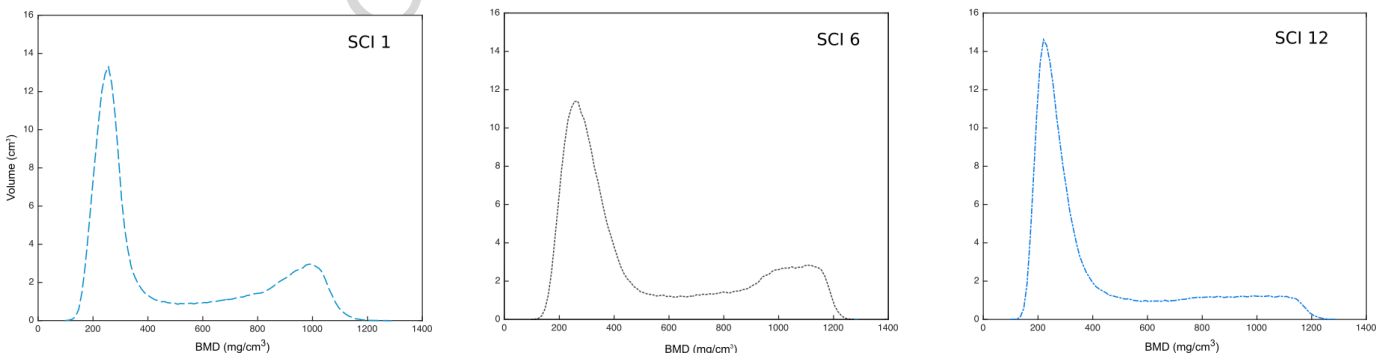

Figure 4: Individual BMD distributions in the tibia models of two male (SCI1, SCI 6) and one female (SCI 12) subjects with early SCI who already exhibit a move away from the healthy "double-peak" BMD distribution, showing instead a pattern that is more typical of established SCI: (i) a trabecular peak skew, and (ii) a diminishing cortical peak.

4. DISCUSSION

By producing a 3D representation of pQCT voxels along the length of the tibia, a "double peak" curve of BMD distribution is obtained for a typical, healthy bone. The most striking variability within the SCI group occurs in the cortical BMD region rather than the trabecular BMD region, which has not been documented previously. To date, most studies have focused on using finite element modelling techniques to associate the risk of fracture with the overall mechanical integrity of the bone. However, such methods are time consuming. Analysing the BMD distribution of the voxels - without the need for finite element modelling - provides a more time-efficient method to estimate the mechanical strength of the bone, where segmentation and 3D modelling can be done using semi-automated methods. The methodology and findings presented in this paper can be compared with the results of computational models **[7]** and experimental cadaveric validation **[16]** demonstrating that bones that have a higher percentage of cortical bone are less susceptible to fractures. By analysing the double peak curve presented in the paper, it would be possible to identify the subjects at risk of shaft fractures, as well as epiphyseal ones. Given the fact that most of the denser cortical bone can be found in the diaphysis it can be assumed that the bones with lower (or absent) cortical peaks would be more susceptible to fracture due to shear and torsional loads. Only by creating patient-specific models is it possible to make assumptions about the individual patient's fracture risk. Even though between-group comparisons highlight a general trend in patterns of cortical BMD distribution after SCI, fracture prevention based on individualised bone models would most benefit patients who deviate from this trend.

The comparison of BMD distributions between healthy controls, subjects with early SCI (<4 years since injury) and those with established SCI (≥ 4 years) confirms a general, time-dependent nature of the disuse-related bone loss to which people with chronic SCI are prone. Although small numbers of subjects were included in this cross-sectional study, the observations from patient-specific modelling of the tibia in group with SCI illustrate some interesting patterns. Overall trends, from healthy AB to those with early SCI and those with established SCI, suggest clear and progressive changes in the cortical BMD ranges and in the trabecular BMD ranges. The clear decreases in peak trabecular BMD values are as expected, as the most fracture-prone sites in the tibia in chronic SCI are the epiphyses **[13]**. In a related paper, the results of finite-element simulations (based on individual 3D models of the tibia) confirm the types of loading that typically lead to fracture in chronic SCI **[7]**. Torsion and bending loading scenarios lead to epiphyseal fractures in the proximal and distal tibia, which are the weakest regions of the bone in chronic SCI. However, the findings of the follow-on study described here show that, even by only analysing the patient-specific BMD distribution within the bone, it is possible to obtain information about the mechanical integrity of the bone, without having to go through time-consuming finite element simulation methods **[16]**. In general, the epiphyseal regions have been confirmed to be the weakest – i.e. the distal and proximal tibia. However, in addition, individuals exhibiting low BMD in the diaphysis as well as the epiphysis also appear to be at increased risk of fracture in the main shaft of the bone, when compared to an age- and sex-matched, healthy control subject's tibia **[7,16]**.

In our personalised 3D models of BMD distribution, a healthy "double-peak" BMD distribution in AB and most subjects in the early stages of SCI is suggestive of similar bone volumes in the trabecular and cortical BMD ranges. The move away from this double-peak BMD distribution towards a tibia that is predominantly composed of low-BMD trabecular bone and very little high-BMD cortical bone may be indicative of a weakening diaphysis in these individuals. The potential weakening of the diaphysis with a diminishing cortical BMD peak would need to be confirmed using finite element model simulations, as described in [7] and validated in [16] by Gislason et al..

The value of the patient-specific models is in identifying individuals with significantly affected cortical BMD distributions, specifically a reduced/absent cortical density peak, with an increased proportion of low-BMD trabecular bone instead. This could be indicative of a weakening tibial shaft (diaphysis). The data from the subject-specific models suggest that time since injury must not be the sole consideration when clinicians make decisions about osteoporosis- and fracture-prevention management in individual patients after SCI. Coupaud *et al.* **[3]** and Varzi *et al.* **[9]** have already shown considerable variability in rates of bone loss in patients in the early phases of SCI (first 12 months), and this is likely to continue to be relevant years after SCI. On the positive side, some patients with established SCI such as SCI 5 (23 years post-injury) show a normal BMD double-peak, thus a tibial diaphysis that has similar BMD distribution to a healthy AB person.

In contrast to previous studies of disuse osteoporosis after SCI, this pQCT investigation does not simply focus on general trends of bone loss in the SCI population, highlighting instead the inter-subject differences **[17,18]**. Comparison of BMD distribution and bone geometry between subjects with SCI and healthy AB controls highlights the abnormalities in BMD in some subjects with SCI. Although larger numbers of subjects would be required to determine the true extent of the variability in patterns of bone loss after SCI, with patients assessed at regular intervals in a prospective longitudinal study to follow each patient over a number of years, this study suggests that time since injury may not be a robust predictor of those likely to have an abnormal BMD distribution. Some individuals with established SCI (≥ 4 years post-injury) who are expected to have reached their steady-state values (according to Eser et al.'s pQCT-derived time course descriptions **[1]**) still show a healthy double-peak BMD distribution, similar to AB control subjects (e.g. SCI 5, 23 years post-injury); others with early SCI already have an abnormal distribution of trabecular and cortical BMD, whether male (e.g. SCI 1 and SCI 6) or female (SCI 12).

In some cases, early decreases in cortical BMD may be transient. Indeed, the data overall suggest a transient increase in the absolute area under the cortical region of the curve ("cortical AUC"), as well as that cortical AUC as a percentage of total AUC, during early SCI. This may coincide with a period of increased cortical bone remodelling in the first few years after injury. Large inter-subject variability in measures describing the cortical region of the BMD distribution curve in those with established SCI illustrates the value of subject-specific BMD distribution models in this patient cohort. Descriptions of the variability in cortical BMD distribution in the tibial shaft of individuals with

SCI, irrespective of time since injury, has not until now been documented in the literature, but may have implications for osteoporosis management in this population.

Due to the different spatio-temporal patterns of bone loss, the most appropriate musculoskeletal rehabilitation approach for osteoporosis management is likely to vary between patients. Findings from our personalised 3D models of the tibia lend support to the hypothesis that the variation in specific patterns of bone loss resulting from injury and disuse are likely to lead to changes in the level and location of weak regions along the tibia in different patients with SCI. Personalised musculoskeletal rehabilitation interventions, targeted at weak regions of the long bones in the paralysed limbs of patients with SCI, theoretically have the potential to stimulate bone formation in the specific parts of the skeleton that require strengthening to reduce the risk of fracture. However, the suggestion of using the 3D models described here to inform the design of rehabilitation interventions, tailored to the individual patient's needs for strengthening of the long bones, is currently speculative. Furthermore, there is only equivocal evidence for specific forms of physical intervention (e.g. electrically-stimulated exercise) having any potential to encourage local bone formation in the paralysed limbs **[19,20,21]**, let alone doing so at sufficient levels to reduce fracture risk in the long bones of people with chronic SCI in the long term. A longitudinal intervention and imaging study that makes use of these 3D models for patient-specific rehabilitation design would be required to evaluate this proposed approach.

Limitations of our study result from the cross-sectional design of the study, and the fact that no power calculations were performed to determine the ideal sample sizes for the SCI and control groups. Although the gender and age profiles were similar between the two groups, the numbers of female subjects were small, especially the control group which only included one post-menopausal woman, compared to three in the SCI group (albeit of similar age). The main technical limitations of the study relate to sources of error in stacking the images along the length of the tibia, due to: (i) spasms during scanning sessions leading to misalignment of images; (ii) scanning each tibia in two halves (distal portion, followed by proximal portion) combined with a method of aligning the images based on fiducial marker position, (iii) interpolation between images slices, (iv) partial volume effects. However, the use of a fiducial marker rod along the subject's lower leg and the removal of the outer layer (cortical shell) of bone prior to analysis of epiphyseal bone slices have reduced the impact of these problems. Another limitation, relating to BMD calculations in the epiphyses of the tibia in the SCI group, is in the image analysis and threshold-based method for identifying the periosteal surface and calculating trabecular and total BMD at these sites (epiphyses – at 4% and 96% of total bone length). The use of the manufacturer's default peel-mode P1 for trabecular BMD calculations rather than a user-defined threshold peel-mode P2 can lead to errors in BMD estimation at the epiphyses after SCI, where the cortical shell has thinned and the set threshold can fail to detect the periosteal edge adequately. This occurs because pQCT voxels within the cortex are removed if they have a lower attenuation coefficient than the set peel thresholds (in our study: 180 mg/cm^3 for distal tibia, 150 mg/cm^3 for proximal tibia) **[14]**. However, using this default peel mode (P1) allows for direct comparison with data from most published pQCT studies for the SCI patient group (and other relevant populations). Furthermore, in our experience, reducing the threshold manually for better bone edge detection typically only changes trabecular BMD calculations by a small amount (2-5 mg/cm^3).

5. CONCLUSIONS

The value of the information gleaned from multi-slice pQCT (combined with interpolation between slices) to create individualised tibia models is that the subject-specific model outputs give an instant visual representation of any unusual bone material distribution. Although group comparisons describe the trends in changes in BMD distribution after SCI, away from the healthy 'double-peak' BMD distribution and more towards a low-BMD skew in the trabecular bone BMD range (around 200-300 mg/cm^3), attention should be paid to each patient's own BMD distribution and the extent of their deviation from the normal double-peak pattern. In patients who seem to lose vast amounts of high-density cortical bone (as evidenced from a diminishing/absent peak in the cortical BMD range), the predominance of low-density bone throughout the tibia may represent a weaker diaphysis and higher risk of shaft fractures in those individuals.

CONFLICTS OF INTEREST:

None

ACKNOWLEDGEMENTS:

We would like to thank all the study participants for taking part, and the staff at the Queen Elizabeth National Spinal Injuries Unit for their assistance with this study. This research did not receive any specific grant from funding agencies in the public, commercial, or not-for-profit sectors. However, we acknowledge the Royal Society of Edinburgh for funding an international exchange visit from KS to Glasgow, and the Glasgow Research Partnership in Engineering, the Centre for Excellence in Rehabilitation Research and NHS Greater Glasgow & Clyde R&D for additional support.

REFERENCES:

[1] Eser P., Frotzler A., Zehnder Y., Wick L., Knecht H., Denoth J. and Schiessl, H. Relationship between the duration of paralysis and bone structure: a pQCT study of spinal cord injured individuals. *Bone* 2004, 34(5): 869–880. DOI: 10.1016/j.bone.2004.01.001

[2] Coupaud S., McLean A.N. and Allan D.B. Role of peripheral Quantitative Computed Tomography in identifying disuse osteoporosis in paraplegia. *Skeletal Radiol* 2009, vol. 38 (10): 989-995. DOI: 10.1007/s00256-009-0674-1

[3] Coupaud S., McLean A.N., Purcell M., Fraser M.H. and Allan D.B. Decreases in bone mineral density at cortical and trabecular sites in the tibia and femur during the first year of spinal cord injury. *Bone* 2015, 74: 69-75. DOI: 10.1016/j.bone.2015.01.005

[4] Frotzler A., Berger M., Knecht H. and Eser P. Bone steady-state is established at reduced bone strength after spinal cord injury: A longitudinal study using peripheral quantitative computed tomography (pQCT). *Bone* 2008, 43: 549–555. DOI: 10.1016/j.bone.2008.05.006

[5] McCarthy I.D., Bloomer Z., Gall A., Keen R. and Ferguson-Pell M. Changes in the structural and material properties of the tibia in patients with spinal cord injury. *Spinal Cord* 2012; 50(4): 333-337. DOI: 10.1038/sc.2011.143

[6] Coupaud S., McLean A.N., Lloyd S. and Allan D.B. Predicting patient-specific rates of bone loss at fracture-prone sites after spinal cord injury. *Disabil Rehabil* 2012, vol 34 (26): 2242-2250. DOI: 10.3109/09638288.2012.681831

[7] Gislason M., Coupaud S., Sasagawa K., Tanabe Y., Purcell M., Allan D.B. and Tanner K.E. Prediction of risk of fracture in the tibia due to altered bone mineral density distribution resulting from disuse: a finite element study. *Proc IMecE Part H: J Eng Med* 2014, 228: 165-174. DOI: 10.1177/0954411914522438

[8] Findlay C. (2012) Image analysis tool for the characterisation of bone turnover in the appendicular skeleton. *Doctoral thesis*, University of Glasgow (Glasgow, U.K.).

[9] Varzi D., Coupaud S., Purcell M., Allan D.B., Gregory J.S. and Barr R.J. Bone morphology of the femur and tibia captured by statistical shape modelling predicts rapid bone loss in acute spinal cord injury patients. *Bone* 2015; 81: 495-501. DOI: 10.1016/j.bone.2015.08.026

[10] Vestergaard P., Krogh K., Rejnmark L. and Mosekilde L. Fracture rates and risk factors for fractures in patients with spinal cord Injury. *Spinal Cord* 1998, 36 (11): 790-796. DOI: 10.1038/sj.sc.3100648

[11] Eser P., Frotzler A., Zendher Y. and Denoth J. Fracture Threshold in the Femur and Tibia of People With Spinal Cord Injury as Determined by Peripheral Quantitative Computed Tomography. *Arch Phys Med Rehabil* 2005, 86: 498-504. DOI: 10.1016/j.apmr.2004.09.006

[12] Lazo M.G., Shirazi P., Sam M., Giobbie-Hurder A., Blacconiere M.J. and Muppidi M. Osteoporosis and risk of fracture in men with spinal cord injury. *Spinal Cord* 2001, 39: 208-214. DOI: 10.1038/sj.sc.3101139

[13] Frotzler A., Cheikh-Sarraf B., Pourtehrani M., Krebs J. and Lippuner K. Long-bone fractures in persons with spinal cord injury. *Spinal Cord* 2015, 53(9): 701-704. DOI:10.1038/sc.2015.74

[14] Giangregorio L.M., Gibbs J.C. and Craven B.C. Measuring muscle and bone in individuals with neurologic impairment; lessons learned about participant selection and pQCT scan acquisition and analysis. *Osteoporos Int* 2016; 27: 2433-2446. DOI: 10.1007/s00198-016-3572-0.

[15] Pauchard Y., Liphardt A.-M., Macdonald H.M., Hanley D.A. and Boyd S.K. Quality control for bone quality parameters affected by subject motion in high-resolution peripheral quantitative computed tomography. *Bone* 2012, 50: 1304-1310. DOI: 10.1016/j.bone.2012.03.003

[16] Gislason M., Coupaud S., Fogg Q.A., McNally S., Purcell M., Sasagawa K., Tanabe Y. and Tanner K.E. Validation of finite element models predicting fracture in the osteoporotic tibia. In: Proc. of the XXV Congress of the International Society of Biomechanics (Glasgow, UK) July 2015

[17]Rittweger J., Goosey-Tolfrey V.L., Cointry G. and Ferretti J.L. Structural analysis of the human tibia in men with spinal cord injury by tomographic (pQCT) serial scans. *Bone* 2010; 47: 511-518. DOI: 10.1016/j.bone.2010.05.025

[18]Capozza R., Feldman S., Mortarino P., Reina P., Schiessl H., Rittweger J., Ferretti J.L. and Cointry G.R. Structural analysis of the human tibia by tomographic (pQCT) serial scans. *J Anatomy* 2010, 216(4): 470–481. DOI: 10.1111/j.1469-7580.2009.01201.x

[19]Dudley-Javoroski S. and Shields R.K. Dose estimation and surveillance of mechanical loading interventions for bone loss after spinal cord injury. *Phys Therapy* 2008, 88(3): 387-396. DOI: 10.2522/ptj.20070224

[20]Dudley-Javoroski S. and Shields R.K., Asymmetric bone adaptations to soleus mechanical loading after spinal cord injury. *J Muscuoloskel Neuronal Interact* 2008, 8(3): 227-238.

[21]Frotzler A., Coupaud S., Perret C., Kakebeeke T.H., Hunt K.J., Donaldson N.D. and Eser P. High-volume FES-cycling partially reverses bone loss in people with chronic spinal cord injury. *Bone* 2008, 43:169-76. DOI: 10.1016/j.bone.2008.03.004

HIGHLIGHTS

- Bone scans were performed on 13 subjects with spinal cord injury (SCI) and 7 able-bodied (AB) subjects.
- Subject-specific models were created, showing three dimensional bone mineral (BMD) distribution in the tibia.
- Chronic SCI is characterised by a greater volume of low BMD trabecular bone, and typically less high BMD cortical bone, compared with healthy AB controls.
- Inter-subject variability in BMD distribution (especially cortical BMD) in the tibia after SCI is high.
- The study findings may have implications for determining fracture susceptibility after SCI, on a case-by-case basis.